Stable and Robust Discrete-time Tracking Control of Unmanned Vehicles Using a Finite-Time Stable Disturbance Observer

Reza Hamrah[1] and Amit Kumar Sanyal[1]

[1]Syracuse University Department of Mechanical and Aerospace Engineering

June 5, 2023

Abstract

This work provides an asymptotically stable and robust tracking control scheme using a finite-time stable disturbance observer in the feedback loop, for an unmanned vehicle modeled as a rigid body. The dynamics of the system is discretized using a Lie group variational integrator in the form of a "gray box" dynamics model that also accounts for unknown additive disturbance force and torque. These disturbance terms are estimated using the finite-time stable disturbance observer in real-time and then compensated by the control scheme. The stability analysis for translational and rotational motions is carried out separately. It is shown that the discrete-time control laws achieve asymptotically stable tracking of the reference position and attitude trajectories.

JOURNAL PAPER

Stable and Robust Discrete-time Tracking Control of Unmanned Vehicles Using a Finite-Time Stable Disturbance Observer

Reza Hamrah | Amit K. Sanyal*

Department of Mechanical and Aerospace Engineering, Syracuse University, New York, USA

Correspondence
*Amit K. Sanyal, Department of Mechanical and Aerospace Engineering, Syracuse University, Syracuse, NY 13244, USA. Email: aksanyal@syr.edu

Present Address
Department of Mechanical and Aerospace Engineering, Syracuse University, Syracuse, NY 13244, USA

Summary

This work provides an asymptotically stable and robust tracking control scheme using a finite-time stable disturbance observer in the feedback loop, for an unmanned vehicle modeled as a rigid body. The dynamics of the system is discretized using a Lie group variational integrator in the form of a "gray box" dynamics model that also accounts for unknown additive disturbance force and torque. These disturbance terms are estimated using the finite-time stable disturbance observer in real-time and then compensated by the control scheme. The stability analysis for translational and rotational motions is carried out separately. It is shown that the discrete-time control laws achieve asymptotically stable tracking of the reference position and attitude trajectories.

KEYWORDS:
geometric mechanics, geometric and nonlinear controls, nonlinear observer design

1 | INTRODUCTION

Unmanned vehicles have gained a lot of attention due to their increasing use in several applications including security and monitoring, infrastructure inspection, agriculture, wildland fire management, package delivery, remote sensing, and underwater and space exploration. With improved onboard sensing and processing capabilities, the autonomy of these vehicles and their use in challenging applications have also increased. Challenges in these applications of unmanned vehicles arise mainly due to external uncertainties like atmospheric turbulence, the presence of unknown natural or human-made structures, and wind or water currents. For example, the use of unmanned aerial vehicles (UAVs) in monitoring wildland fires makes the vehicles subject to unsteady and turbulent airflow, higher temperatures, and variable air density. These effects lead to uncertainties in the flight dynamics, affecting both the translational and rotational motion, which in turn can lead to adverse effects on the performance of these vehicles [1,2]. Therefore, it becomes critical in challenging applications to ensure nonlinearly stable and robust operations, with guaranteed stability properties.

Most unmanned vehicles can be modeled as rigid bodies with six degrees of freedom, where the control inputs act on the three degrees of rotational motion and one degree of translational motion in a vehicle body-fixed coordinate frame. This actuation model is applicable to a wide range of unmanned vehicles, including fixed-wing and rotorcraft unmanned aerial vehicles, underwater vehicles, and spacecraft, which possess body-fixed actuators that provide a single body-fixed thrust direction and three body-fixed torque components. However, the autonomous operation of such vehicles presents three primary challenges: (a) the feedback control system needs to be nonlinearly stable to enable large maneuvers that may be required for collision avoidance, for example; (b) control schemes have to be robust to unknown disturbance forces and torques for the safety and reliability of operations; and (c) control laws need to be computationally lightweight and designed in discrete time to facilitate onboard implementation in real time [3], as well as enhance robustness and stability against control disturbances. These challenges motivate the

objective of this paper, which is *to develop a stable and robust data-driven feedback control scheme in the presence of unknown disturbance inputs for unmanned vehicles in three-dimensional motion. The proposed scheme identifies (unknown) dynamic disturbance inputs by analyzing (known) applied control inputs and real-time sensed outputs, providing robust feedback control to compensate for these disturbances.*

An effective technique to maintain the control performance in the face of disturbances and uncertainties is the active disturbance rejection control (ADRC)[4]. In this technique, the first step involves estimating the unknown disturbance using disturbance estimation techniques. This estimated disturbance is then incorporated into the control design to effectively reject the disturbance. Extended state observer (ESO) is a technique widely employed for disturbance estimation and rejection. It has been applied in various studies to enhance control performance in different domains including trajectory tracking control using an asymptotically stable linear ESO[5], tracking control using fixed-time stable disturbance observer and fault-tolerance mechanisms[6], and finite-time stable (FTS) ESO[7,8]. Researchers have also utilized ESOs in combination with other control strategies such as incremental nonlinear dynamics inversion (INDI) control and sliding-mode observer (SMO)[9]. Furthermore, adaptive variations of ESO, such as the adaptive super-twisting ESO, have been proposed[10,11]. Apart from ESO, other techniques such as the disturbance observer (DO)[12,13,14,15] and unknown input observer(UIO)[16], can also be used to estimate disturbances within a disturbance rejection control framework. DOs are advantageous in the design of robust control. They are commonly used to estimate uncertainties in nonlinear systems as they are intuitive in design and possess a simple structure. Their main role is to estimate the disturbance inputs (uncertainties) acting on the dynamics. This helps in creating a modular design of controllers where a nominal controller can be designed for the nominal plant without disturbance inputs, while disturbance estimates from the DO are used to compensate them[17]. In this regard, a control design using a nonlinear DO offers several advantages over other control methods such as $\mathcal{H}_\infty$ control, adaptive control, or sliding mode control. These advantages include its ability to handle unknown or time-varying disturbances, faster and more accurate disturbance rejection, not requiring exact knowledge of the system model, and simpler implementation in a more computationally efficient manner. The pose tracking controller given here uses a finite-time stable and Hölder-continuous disturbance observer (FTS-DO)[18]. This FTS-DO was used in our recent work[19] for stable and robust position tracking control. In this work, we design discrete-time tracking control laws that leverage the FTS-DO design to compensate for disturbance force and disturbance torque inputs acting on the vehicle's body, for position and attitude tracking control on the Lie group of rigid body motions, SE(3). This FTS-DO has a faster convergence rate and better disturbance rejection abilities than conventional nonlinear DO. It is also designed to converge in a finite time period shorter than the settling time of the controller, resulting in faster disturbance rejection and improved stability. The use of Hölder-continuous FTS-DO in the proposed tracking control design can also avoid chattering resulting from measurement noise and unknown disturbances to dynamics in other stabilization methods like sliding mode[20,21]. It also provides greater design freedom for the nominal system's controller design. Therefore, DO-based techniques provide a feasible way to improve robustness and deal with disturbances or system uncertainties in real time.

In this work, we design pose (position and orientation) tracking feedback control laws for underactuated vehicles, which ensures asymptotically stable convergence of the vehicle's pose to the desired trajectory in the presence of unknown dynamic disturbance inputs. The discrete-time dynamics model is a "gray box" model that is discretized using the framework of discrete geometric mechanics and obtained in the form of a Lie group variational integrator (LGVI)[22,23,24]. The advantages of LGVIs are: (1) they discretize the motion on the Lie group without the need for local maps or projection, and (2) they are variational in nature which implies preservation of energy-momentum properties of the continuous dynamics[25,26]. It combines a physics-based model that accounts for known physics, with unknown disturbance inputs due to environmental effects. The control inputs also compensate for the disturbance force and disturbance torque acting on the vehicle using estimates of such inputs obtained from a Disturbance Observer design. The control laws are designed in discrete time for ease of onboard computer implementation, and it is shown to be stable and robust to the control disturbance in real time. As a result, this design meets the technical challenges stated earlier, i.e., of nonlinear stability and robustness to disturbances. A schematic block diagram of the proposed design is given in Fig. 1.

A brief outline of this paper is as follows. In Section 2, we provide preliminary concepts and notation on rigid body motion. The formulation of the disturbance observer is stated briefly in Section 3. Section 4 obtains the pose tracking control laws for stable translational motion control, which is used to generate the reference attitude trajectory[27]. The asymptotically stable attitude tracking control law is then obtained in discrete time in Section 5. Numerical simulation results based on the LGVI model and the discrete-time observer and obtained control laws are demonstrated in Section 6. We conclude the paper in Section 7, by summarizing the results and highlighting directions for further research.
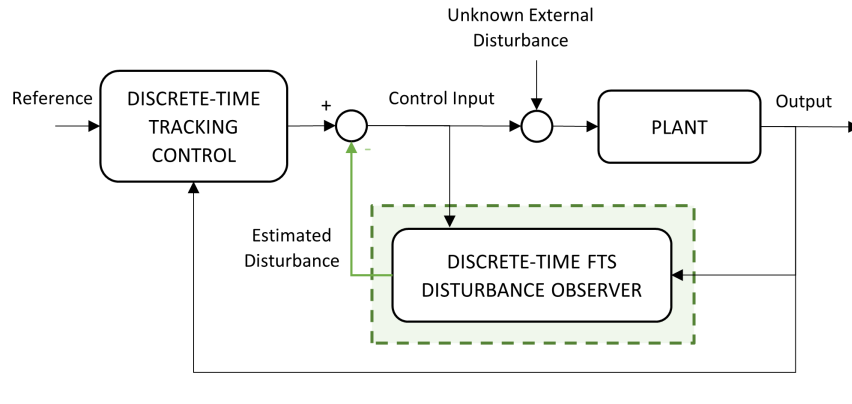
FIGURE 1 FTS disturbance observer integrated with a feedback tracking controller

2 | PROBLEM FORMULATION

The set of possible configurations for rigid body motions is the Lie group SE(3). The group SE(3) is the semi-direct product of $\mathbb{R}^3$ and the special orthogonal group of rigid body orientations SO(3), i.e., SE(3) $= \mathbb{R}^3 \rtimes$ SO(3)[28,29], where the special orthogonal group of rigid body rotation, SO(3)[30], is defined as

$$\text{SO(3)} = \left\{ R \in \mathbb{R}^{3\times3}, \ R^{\mathsf{T}}R = RR^{\mathsf{T}} = \mathbf{I}, \ \det(R) = 1 \right\}.$$

Both SO(3) and SE(3) are matrix Lie groups under matrix multiplication. The Lie algebra (tangent space at identity) of SO(3) is denoted $\mathfrak{so}(3)$ and defined as,

$$\mathfrak{so}(3) = \left\{ S \in \mathbb{R}^{3\times3} \mid S + S^{\mathsf{T}} = 0 \right\},$$

$$S = \mathrm{s}^{\times} = \begin{bmatrix} 0 & -\mathrm{s}_3 & \mathrm{s}_2 \\ \mathrm{s}_3 & 0 & -\mathrm{s}_1 \\ -\mathrm{s}_2 & \mathrm{s}_1 & 0 \end{bmatrix}.$$

Here $(.)^{\times} : \mathbb{R}^3 \rightarrow$ SO(3) denotes the bijective map from three dimensional Euclidean space to $\mathfrak{so}(3)$. For a vector $\mathrm{s} = [\mathrm{s}_1 \ \mathrm{s}_2 \ \mathrm{s}_3]^{\mathsf{T}} \in \mathbb{R}^3$, the matrix $\mathrm{s}^{\times}$ represents the vector cross product operator, that is $\mathrm{s} \times r = \mathrm{s}^{\times}r$, where $r \in \mathbb{R}^3$. The inverse of $(.)^{\times}$ is denoted by $\mathrm{vex}(.) : \mathfrak{so}(3) \rightarrow \mathbb{R}^3$, such that $\mathrm{vex}(a^{\times}) = a$, for all $a^{\times} \in$ SO(3).

The pose of a rigid body is given by its position vector, denoted as b, which specifies the vector from the origin of an inertial coordinate frame $\mathcal{I}$ to the origin of a body-fixed coordinate frame $\mathcal{B}$, and its attitude, represented by a rotation matrix R that relates the body-fixed frame $\mathcal{B}$ to the inertial frame $\mathcal{I}$. Together, the pose of the vehicle can be represented in matrix form as

$$\mathrm{g} = \begin{bmatrix} R & b \\ 0 & 1 \end{bmatrix} \in \text{SE(3)}, \tag{1}$$

2.1 | System Kinematics and Dynamics

The instantaneous pose is compactly represented by $\mathrm{g} = (b, R) \in$ SE(3). Denoting the time derivative by $(\dot{\ })$, the vehicle's kinematics is given by:

$$\begin{cases} \dot{b} = \upsilon = Rv, \\ \dot{R} = R\Omega^{\times}, \end{cases} \tag{2}$$

where $\upsilon \in \mathbb{R}^3$ and $v \in \mathbb{R}^3$ denote the translational velocity in frames $\mathcal{I}$ and $\mathcal{B}$, respectively, and $\Omega \in \mathbb{R}^3$ is the angular velocity in frame $\mathcal{B}$. The dynamics of an underactuated vehicle modeled as a rigid body with a body-fixed plane of actuators is given by:

$$\begin{cases} m\ddot{b} = m\dot{\upsilon} = mge_3 - (\varphi + \phi^d), \\ J\dot{\Omega} = -\Omega^{\times}J\Omega + \tau + \tau^d, \end{cases} \tag{3}$$

where $e_3 = [0\ 0\ 1]^T$ is the third standard basis of $\mathbb{R}^3$, g denotes the acceleration due to gravity, and $m \in \mathbb{R}^+$ and $J = J^T \in \mathbb{R}^{3 \times 3}$ are the mass and inertia matrix of the vehicle, respectively. $\varphi = f R e_3$ is the control force vector acting on the body, and its magnitude is $f \in \mathbb{R}$, which is designed as a feedback control law. $\tau \in \mathbb{R}^3$ is the control torque created by the rotors, and the disturbance force and torque vectors are denoted ϕ^d and τ^d, respectively, which are mainly due to unsteady aerodynamics.

The vehicle's kinematics and dynamics equations of motion are discretized using the framework of discrete geometric mechanics here, and the resulting discrete-time equations of motion are obtained in the form of LGVI[31]. Consider a time interval $[t_0, T] \in \mathbb{R}^+$ separated into N equal-length subintervals $[t_k, t_{k+1}]$ for $k = 1, 2, \dots, N$ with $t_N = T$ and $\Delta t = t_{k+1} - t_k$ is the time step size. Then, the discretized equations of motion using LGVI are obtained as

$$\begin{cases} b_{k+1} = b_k + \Delta t R_k v_k, \\ R_{k+1} = R_k \exp(\Delta t \Omega_k^\times), \\ m v_{k+1} = m F_k^T v_k + m g R_{k+1}^T e_3 - \Delta t(f_k e_3 + \phi_k^d), \\ J \Omega_{k+1} = F_k^T J \Omega_k + \Delta t(\tau_k + \tau_k^d), \end{cases} \tag{4}$$

where

$$F_k = R_k^T R_{k+1} = \exp(\Delta t \Omega_k^\times) \in SO(3), \tag{5}$$

and the matrix exponential in (4) is evaluated using Rodrigues' formula for numerical efficiency:

$$\exp(\Delta t \Omega^\times) = I + \frac{\sin \|\Delta t \Omega\|}{\|\Delta t \Omega\|}(\Delta t \Omega^\times) + \frac{1 - \cos \|\Delta t \Omega\|}{\|\Delta t \Omega\|^2}(\Delta t \Omega^\times)^2. \tag{6}$$

The derivation of these equations requires the use of the discrete Lagrange d'Alembert principle to get the equations of motion for a rigid body. For a detailed derivation, the reader is directed to the previous works[22,23].

2.2 | Tracking Error Kinematics and Dynamics

A smooth position trajectory that is continuous and twice differentiable (i.e., $b^r(t) = C^2(\mathbb{R}, \mathbb{R}^3)$), where $b^r(t)$ gives the desired position trajectory on $\mathbb{R}^3$ through multiple waypoints, can be generated using several techniques reported in the literature such as Hybrid A*[32,33], LQR-based trajectories[34,35,36], or other reported schemes[37]. Once the desired position trajectory is generated for the underactuated vehicle with a body-fixed thrust direction, a desired attitude trajectory $R^r(t)$ is generated such that the position trajectory is tracked. This desired attitude trajectory is generated using the desired control force vector derived from an outer loop position tracking scheme (explained in Section 4). The method for generating the desired attitude trajectory is described in previous works[27,38]. Subsequently, the inner loop attitude control design is employed to track the generated desired attitude trajectory.

Let $g^r(t) \in SE(3)$ be the reference pose, v^r and v^r denote the reference translational velocity in the inertial frame $\mathcal{I}$ and the body frame $\mathcal{B}$, respectively, and Ω^r denote the body's reference angular velocity in the body frame. Then, tracking error is given by

$$h = (g^r)^{-1} g = \begin{bmatrix} Q & x \\ 0 & 1 \end{bmatrix} \in SE(3), \tag{7}$$

where $Q = (R^r)^T R$ is the attitude tracking error, and $x = (R^r)^T(b - b^r) = (R^r)^T \tilde{b}$ is the position tracking error, both in the reference body fixed frame. Also, the angular velocity tracking error is given by

$$\omega = \Omega - Q^T \Omega^r. \tag{8}$$

Now, using the LGVI discretized equations of motion (4) and combining it with the tracking error in (7), we get the discrete-time pose error kinematics and dynamics in the form of LGVI[23,24] as

$$\begin{cases} \tilde{b}_{k+1} = \tilde{b}_k + \Delta t \tilde{v}_k, \\ R_{k+1} = R_k F_k, \\ m \tilde{v}_{k+1} = m v_k + \Delta t\, m g\, e_3 - \Delta t(\varphi_k + \phi_k^d) - m v_{k+1}^r \\ J \omega_{k+1} = F_k^T J \Omega_k - J Q_{k+1}^T \Omega_{k+1}^r + \Delta t(\tau_k + \tau_k^d), \end{cases} \tag{9}$$

where $v_{k+1} = \tilde{v}_{k+1} + v_{k+1}^r$, $F_k \approx \exp(\Delta t \, \Omega_k^\times)$, and Q_{k+1} is the attitude tracking error kinematics in discrete form as:

$$Q_{k+1} \approx Q_k \left[I + \frac{\Delta t}{2} (\omega_{k+1} + \omega_k)^\times \right]. \tag{10}$$

3 | FINITE-TIME STABLE DISTURBANCE OBSERVER

The disturbance observer discussed in this section builds on our recent work [18] which develops a finite-time stable disturbance observer (FTS-DO) in discrete time for a generalized 6-DoF system of an unmanned vehicle. The unknown dynamics of the vehicle are the disturbance force and torque. The disturbance observer runs in the inner loop in the control system architecture and the estimated disturbances will be used in the tracking controller to attenuate the unknown disturbance force and torque in the dynamics model. The unknown disturbance inputs $\chi_k = [\phi_k^d, \tau_k^d]^T \in \mathbb{R}^6$ are learned in real time according to the past input-output history. Let us define the error in estimating χ_k as:

$$e_k^\chi := \hat{\chi}_k - \chi_k. \tag{11}$$

Also, the first-order finite difference of the unknown dynamics, χ_k, is denoted as:

$$\Delta \chi_k := \chi_k^{(1)} = \chi_{k+1} - \chi_k \tag{12}$$

The disturbance estimate, $\hat{\chi}_k = [\hat{\phi}_k^d, \hat{\tau}_k^d]^T \in \mathbb{R}^6$, can be obtained in real-time from the following first-order nonlinearly stable observer. The following two propositions have been used to prove the main result of the FTS-DO design used in this paper. The detailed proof of these two propositions is given in our previous work [18] and omitted here for brevity.

Proposition 1. The nonlinear observer for χ_k given by:

$$\hat{\chi}_{k+1} = \mathcal{D}(e_k^\chi) e_k^\chi + \chi_k, \tag{13}$$

where $\hat{\chi}_0 = \chi_0$ is given and $\mathcal{D} : \mathbb{R}^+ \to \mathbb{R}$ is a Hölder-continuous function that is given by:

$$\mathcal{D}(e_k^\chi) = \frac{((e_k^\chi)^T e_k^\chi)^{1-1/r} - \lambda}{((e_k^\chi)^T e_k^\chi)^{1-1/r} + \lambda}, \tag{14}$$

where $\lambda > 0$ and $r \in (1, 2)$ are constants. The disturbance observer in (13) leads to finite-time stable convergence of the estimation error vector $e_k^\chi \in \mathbb{R}^6$ to a bounded neighborhood of $0 \in \mathbb{R}^6$, where bounds on the neighborhood are obtained from the bounds on $\Delta \chi_k$.

Proposition 2. Consider the nonlinear observer law for the disturbance χ_k given by (13). Let the bound on the first order difference $\Delta \chi_k$ defined by (12) be given by:

$$\|\Delta \chi_k\| \le B^\chi, \tag{15}$$

where $B_\chi \in \mathbb{R}^+$. Then, the observer estimation error e_k^χ is guaranteed to converge to the neighborhood given by:

$$N^\chi := \{ e_k^\chi \in \mathbb{R}^n : \rho(e_k^\chi) \|e_k^\chi\| \le B^\chi \}, \tag{16}$$

for finite $k > N$, $N \in \mathbb{W}$, where

$$\rho(e_k^\chi) := 1 + |\mathcal{D}(e_k^\chi)|. \tag{17}$$

As mentioned in the previous section, the discrete-time stable tracking control scheme [39], which is used here is designed with two loops: an inner loop for attitude control and an outer loop for position control. In the outer loop, given a desired position trajectory in an inertial coordinate frame, the desired control force vector is obtained in discrete time to stabilize the desired trajectory asymptotically. This control force vector expressed in the body-fixed frame is then used to generate a desired attitude trajectory. In the inner loop, to track this desired attitude trajectory, an asymptotically stable attitude tracking scheme is developed and utilized. The outer loop for position tracking also uses a discrete-time asymptotically stable control scheme. In the following sections, these two controllers are integrated into the FTS-DO design presented in this section, as illustrated in the schematic block diagram given in Fig. 2. By doing so, the discrete-time asymptotically stable control laws required for tracking a desired pose trajectory in the presence of control disturbances are obtained.
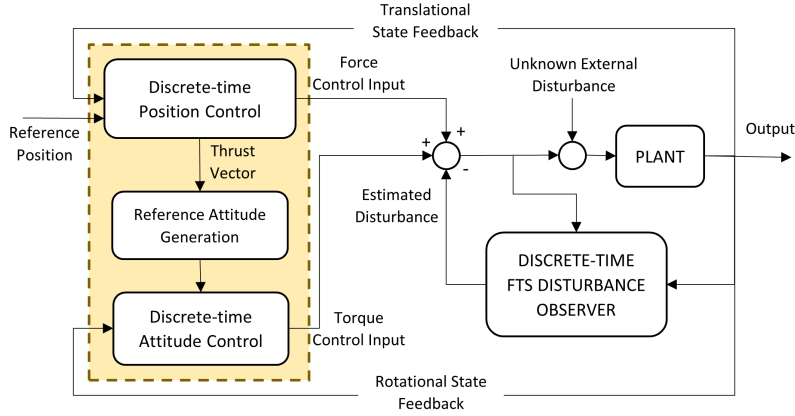
FIGURE 2 Block diagram of integrated position and attitude controllers in the FTS-DO design

4 | DISCRETE-TIME POSITION TRACKING CONTROL DESIGN USING A FTS DISTURBANCE OBSERVER

A position tracking control scheme in discrete time is presented in this section that uses the disturbance estimate provided by the FTS-DO described in the previous section. This controller asymptotically stabilizes the nominal tracking error dynamics (9) without the disturbance force ϕ_k^d or if this disturbance force is constant, and provides ultimate boundedness of tracking errors in the presence of a time-varying disturbance force by compensating the unknown disturbance force using its estimate obtained from the FTS-DO. The following result gives the force control law that is required to track a desired position trajectory in the presence of control disturbance with asymptotic stability. It is a modification of the nominal control law for asymptotically stable position tracking in discrete time obtained in our prior research [39].

Proposition 3. Consider the force control law for reference position trajectory tracking in the presence of unknown disturbance force given by:

$$\varphi_k = \frac{m}{\Delta t}\left\{ \Delta t g e_3 + v_k - v_{k+1}^r - \frac{\Delta t}{m}\widehat{\phi}_k^d - A^{-1}\left[B\tilde{v}_k - \Delta t P \tilde{b}_k\right] \right\}, \tag{18}$$

where

$$A = (M + D + \frac{\Delta t^2}{4}P),$$

$$B = (M - D - \frac{\Delta t^2}{4}P),$$

$M = m\,\mathbf{I}_{3\times 3}$, D and P are positive definite control gain matrices. Then, the tracking error dynamics (9) with an unknown disturbance force ϕ_k^d and the force control law (18) can be expressed as

$$\tilde{v}_{k+1} + \frac{\Delta t}{m}e_k^{\phi} = A^{-1}\left[B\tilde{v}_k - \Delta t P \tilde{b}_k\right], \tag{19}$$

where $e_k^{\phi} = (\widehat{\phi}_k^d - \phi_k^d) \in \mathbb{R}^3$ denotes the error in the estimate of the unknown disturbance force obtained from the first three components of $\widehat{\chi}_k \in \mathbb{R}^6$ as given by the FTS-DO in eq. (13).

Proof. In the case where the estimation of ϕ_k^d is perfect (e.i. $e_k^{\phi} = 0$), from Theorem 3.1 of our asymptotically stable control scheme [39], we have

$$\tilde{v}_{k+1} = A^{-1}\left[B\tilde{v}_k - \Delta t P \tilde{b}_k\right], \tag{20}$$

which is obtained as the error dynamics that guarantees asymptotically stable convergence of the translational tracking errors to zero. More generally, if e_k^{ϕ} reaches a bounded neighborhood of the zero vector in $\mathbb{R}^3$, as would be the case for the disturbance observer (13) applied to a time-varying disturbance, then the disturbed force control law (18) leads to the following feedback dynamics:

$$m\tilde{v}_{k+1} = \Delta t(\phi_k^d - \widehat{\phi}_k^d) + mA^{-1}\left[B\tilde{v}_k - \Delta t P \tilde{b}_k\right], \tag{21}$$

on substitution into the tracking error dynamics equation (9). Rearranging terms in (21), we obtain the error dynamics equation as (19). □

The main result on the ultimate boundedness of reference trajectory tracking errors is as follows.

Theorem 1. *Consider the feedback system consisting of the system dynamics given by* (9), *the observer law* (13), *and the control law* (18). *Let the estimation error for the disturbance force,* e_k^ϕ *be bounded according to:*

$$||e_k^\phi|| \le B^\phi \text{ for } k > N, \tag{22}$$

where $B^\phi \in \mathbb{R}^+$ *and* $N \in \mathbb{W}$ *are known. Then, translational state tracking errors that are given by* $s_k = \left[\tilde{v}_k, \tilde{b}_k\right]^T \in \mathbb{R}^6$ *are guaranteed to converge to the neighborhood given by*

$$\mathcal{N}^s := \left\{ s_k \in \mathbb{R}^6 : \|Z s_k\| \le \Delta t \left(\frac{1}{m} + \frac{\lambda_{\max}(\bar{A})}{\lambda_{\min}(D)}\right) B^\phi \right\} \tag{23}$$

asymptotically, where

$$Z = \left[I - A^{-1}B, \; -\Delta t A^{-1}P\right], \quad \bar{A} = \frac{1}{m}A, \tag{24}$$

and $\lambda_{\max}(\cdot)$ *(* $\lambda_{\min}(\cdot)$ *) denotes the largest (respectively, smallest) eigenvalue of a positive definite matrix.*

Proof. Consider the following candidate Lyapunov function [39], which is the sum of two energy-like terms that are quadratic in position and velocity tracking errors, as

$$V_k(\tilde{b}_k, \tilde{v}_k) = \frac{1}{2}m\tilde{v}_k^\mathrm{T}\tilde{v}_k + \frac{1}{2}\tilde{b}_k^\mathrm{T}P\tilde{b}_k. \tag{25}$$

The discrete-time force control law without the disturbance compensation term[39] is obtained by setting the first difference of the Lyapunov function (25) for the translational motion to be:

$$\Delta V_k = -\frac{1}{2}(\tilde{v}_{k+1} + \tilde{v}_k)^\mathrm{T}D(\tilde{v}_{k+1} + \tilde{v}_k), \tag{26}$$

and using the following approximation:

$$\tilde{b}_{k+1} \approx \tilde{b}_k + \frac{\Delta t}{2}(\tilde{v}_k + \tilde{v}_{k+1}). \tag{27}$$

Re-arranging and expanding (19) in the presence of the disturbance and DO-based compensation, we obtain the following expression:

$$A(\tilde{v}_{k+1} + \frac{\Delta t}{m}e_k^\phi) = B\tilde{v}_k - \Delta t P\tilde{b}_k,$$

$$\Rightarrow (M + D + \frac{\Delta t^2}{4}P)(\tilde{v}_{k+1} + \frac{\Delta t}{m}e_k^\phi) = (M - D - \frac{\Delta t^2}{4}P)\tilde{v}_k - \Delta t P\tilde{b}_k,$$

$$\Rightarrow (M + \frac{\Delta t^2}{4}P)\tilde{v}_{k+1} - (M - \frac{\Delta t^2}{4}P)\tilde{v}_k + \Delta t P\tilde{b}_k = -D(\tilde{v}_{k+1} + v_k) - \frac{\Delta t}{m}(M + D + \frac{\Delta t^2}{4}P)e_k^\phi. \tag{28}$$

The first difference ΔV_k is

$$\Delta V_k = \frac{1}{2}(\tilde{v}_{k+1} + \tilde{v}_k)^\mathrm{T}[m(\tilde{v}_{k+1} - \tilde{v}_k) + \frac{\Delta t}{2}P(\tilde{b}_{k+1} + \tilde{b}_k)]. \tag{29}$$

From the approximation (27), we get

$$m(\tilde{v}_{k+1} - \tilde{v}_k) + \frac{\Delta t}{2}P(\tilde{b}_{k+1} + \tilde{b}_k)$$

$$\approx m(\tilde{v}_{k+1} - \tilde{v}_k) + \Delta t P\tilde{b}_k + \frac{\Delta t^2}{4}P(\tilde{v}_k + \tilde{v}_{k+1})$$

$$= (M + \frac{\Delta t^2}{4}P)\tilde{v}_{k+1} - (M - \frac{\Delta t^2}{4}P)\tilde{v}_k + \Delta t P\tilde{b}_k.$$

Now substituting (28) in the right-hand side of the above expression gives us

$$m(\tilde{v}_{k+1} - \tilde{v}_k) + \frac{\Delta t}{2}P(\tilde{b}_{k+1} + \tilde{b}_k)$$

$$\approx -D(\tilde{v}_{k+1} + \tilde{v}_k) - \frac{\Delta t}{m}Ae_k^\phi \tag{30}$$

$$= -D(\tilde{v}_{k+1} + \tilde{v}_k) - \Delta t \bar{A}e_k^\phi.$$

Substituting (30) into the expression for the first difference (29), we get:

$$\Delta V_k = -\frac{1}{2}(\tilde{v}_{k+1} + \tilde{v}_k)^{\mathrm{T}} D(\tilde{v}_{k+1} + \tilde{v}_k) - \frac{\Delta t}{2}(\tilde{v}_{k+1} + \tilde{v}_k)^{\mathrm{T}} \bar{A} e_k^{\phi}$$

$$\leq \frac{1}{2}(\tilde{v}_{k+1} + \tilde{v}_k)^{\mathrm{T}} D(\tilde{v}_{k+1} + \tilde{v}_k) + \frac{\Delta t}{2}\|\tilde{v}_{k+1} + \tilde{v}_k\|\|\bar{A} e_k^{\phi}\|, \tag{31}$$

where $\bar{A}$ is as defined by (24). More conservative upper bounds on ΔV_k may be obtained using the eigenvalue operators, as

$$\Delta V_k \leq -\frac{1}{2}\lambda_{\min}(D)\|\tilde{v}_{k+1} + \tilde{v}_k\|^2 + \frac{\Delta t}{2}\lambda_{\max}(\bar{A})\|\tilde{v}_{k+1} + \tilde{v}_k\|\|e_k^{\varphi}\|. \tag{32}$$

Setting the above first difference to be non-negative gives (conservative) bounds on the neighborhood to which the tracking error term $\tilde{v}_{k+1} + \tilde{v}_k$ converges, as

$$\|\tilde{v}_{k+1} + \tilde{v}_k\| \leq \frac{\Delta t \lambda_{\max}(\bar{A})}{\lambda_{\min}(D)}\|e_k^{\phi}\|, \tag{33}$$

which, using (27), gives the ultimate boundedness of tracking error term $\tilde{b}_{k+1} - \tilde{b}_k$ as

$$\|\tilde{b}_{k+1} - \tilde{b}_k\| \leq \frac{\Delta t^2 \lambda_{\max}(\bar{A})}{2\lambda_{\min}(D)}\|e_k^{\phi}\|. \tag{34}$$

Finally, from eq. (21), we obtain

$$\tilde{v}_{k+1} + \tilde{v}_k = (I - A^{-1}B)\tilde{v}_k - \Delta t A^{-1} P \tilde{b}_k + \frac{\Delta t}{m} e_k^{\varphi}$$

$$= Z s_k + \frac{\Delta t}{m} e_k^{\phi} \tag{35}$$

Making the further conservative bound for $\|\tilde{v}_{k+1} + \tilde{v}_k\|$ as

$$\|Z s_k\| - \frac{\Delta t}{m}\|e_k^{\phi}\| \leq \|\tilde{v}_{k+1} + \tilde{v}_k\|,$$

and substituting into the inequality (33), and noting that the e_k^{ϕ} be upper bounded by B^{ϕ}, we get the upper bound on $\|Z s_k\|$ as

$$\|Z s_k\| \leq \Delta t \left(\frac{1}{m} + \frac{\lambda_{\max}(\bar{A})}{\lambda_{\min}(D)}\right)\|e_k^{\phi}\|$$

$$\leq \Delta t \left(\frac{1}{m} + \frac{\lambda_{\max}(\bar{A})}{\lambda_{\min}(D)}\right) B^{\phi}$$

as given in (23). $\square$

Note that the above result gives a conservative ultimate bound that is larger than the actual bounds of the neighborhood of the origin that tracking errors may converge to. Tighter bounds can be obtained using other techniques, like LMIs. The following section addresses the stability of the attitude tracking control using the FTS-DO design.

5 | DISCRETE-TIME STABLE ATTITUDE TRACKING CONTROL USING A FTS DISTURBANCE OBSERVER

In this section, we provide an asymptotically stable discrete-time feedback control scheme for attitude motion tracking in the presence of a disturbance torque that is "learned" in real-time by the FTS disturbance observer described in Section 3. It can be implemented on unmanned vehicles that have body-fixed actuators that generate a scalar control thrust force in a body-fixed direction and a three-axis control torque vector, which together actuate four of the six degrees of freedom of a rigid body. This attitude control law asymptotically stabilizes the nominal attitude tracking error dynamics without the disturbance torque τ_k^d in eq. (9) or if this disturbance torque is constant. It provides ultimate boundedness of tracking errors in the presence of a time-varying disturbance torque. The attitude control law is given by the following result and it modifies the asymptotically stable attitude tracking controller in discrete time obtained in our prior research[39], by compensating the unknown disturbance torque using its estimate obtained from the FTS-DO.

Proposition 4. Consider the torque control law using the FTS disturbance observer design is given by

$$\tau_k = \frac{1}{\Delta t}\left\{ J\left(C^{-1}\left[E\omega_k - \Delta t\, k_p\, S_K(Q_k)\right] + Q_{k+1}^T \Omega_{k+1}^r\right) - F_k^T J\Omega_k - \Delta t\, \hat{\tau}_k^d \right\}, \tag{36}$$

where

$$C = (J + L_\omega), \ E = (J - L_\omega), \ k_p > 1,$$

L_ω is a positive definite control gain matrix, and $S_K(Q_k)$ is given by

$$S_K(Q_k) = \text{vex}(KQ_k - Q_k^T K)$$
$$= \Sigma_{i=1}^3 k_i (Q_k^T e_i) \times e_i, \tag{37}$$

where $K = \text{diag}(k_1, k_2, k_3)$ is a diagonal matrix with $k_1 > k_2 > k_3 \geq 1$, and $\hat{\tau}_k^d$ is the estimate of the disturbance torque obtained from the disturbance observer (13). Then, the system dynamics (4) with unknown disturbance torque τ_k^d along with the torque control law (36), satisfies the following estimation error dynamics:

$$\omega_{k+1} + \Delta t \, J^{-1} e_k^\tau = C^{-1} [E\omega_k - \Delta t \, k_p S_K(Q_k)], \tag{38}$$

where $e_k^\tau = (\hat{\tau}_k^d - \tau_k^d) \in \mathbb{R}^3$ denotes the error in the estimate of the unknown disturbance torque obtained from the last three components of $\hat{\chi}_k \in \mathbb{R}^6$ as given by the FTS-DO in eq. (13).

Proof. The proof of this proposition employs a similar methodology as the proof for Proposition 3. By substituting the modified torque control law (36) into the tracking error dynamics (9), the resulting expression (38) is obtained. For brevity, the detailed proof is not presented here. □

The main result on the ultimate boundedness of reference attitude tracking errors is given in the following theorem.

Theorem 2. Consider the system dynamics given by (4), the disturbance observer (13), and the modified torque control (36). Let the estimation error for the disturbance torque, e_k^τ be bounded as:

$$||e_k^\tau|| \leq B^\tau \text{ for } k > N, \tag{39}$$

where $B^\tau \in \mathbb{R}^+$ and $N \in \mathbb{W}$ are known. Then, the angular velocity tracking error given by $\omega_k \in \mathbb{R}^3$ is guaranteed to converge to the neighborhood given by:

$$\mathcal{N}^s := \left\{ \omega_k \in \mathbb{R}^3 : ||\omega_{k+1} + \omega_k|| \leq \frac{\Delta t \lambda_{\max}(\bar{C})}{\lambda_{\min}(L_\omega)} B^\tau \right\} \tag{40}$$

asymptotically, where

$$\bar{C} = J^{-1}C,$$

and $\lambda_{\max}(\cdot)$, and $\lambda_{\min}(\cdot)$ denote the largest and smallest eigenvalue of a positive definite matrix, respectively.

Proof. Consider the following candidate Morse-Lyapunov function, which can be interpreted as the total energy function that is the sum of kinetic and potential energy-like terms for the desired rotational motion:

$$\mathcal{V}_k(Q_k, \omega_k) = \frac{1}{2}\langle J\omega_k, \omega_k \rangle + k_p \langle I - Q_k, K \rangle. \tag{41}$$

where $\langle \cdot, \cdot \rangle$ denotes the trace inner product on $\mathbb{R}^{n_1 \times n_2}$ as

$$\langle A_1, A_2 \rangle := \text{tr}(A_1^T A_2).$$

The discrete-time torque control law in the absence of time-varying disturbance is obtained by analyzing the first difference of the Morse-Lyapunov function (41) for rotational motion[39]. This difference function is represented as

$$\Delta \mathcal{V}_k = \frac{1}{2}(\omega_{k+1} - \omega_k)^T J(\omega_{k+1} + \omega_k) + k_p \langle Q_k - Q_{k+1}, K \rangle, \tag{42}$$

where Q_{k+1} is as given in (10), which can be also written as

$$Q_{k+1} - Q_k \approx \frac{\Delta t}{2} Q_k (\omega_{k+1} + \omega_k)^\times, \tag{43}$$

and allows us to express the change in the potential energy term of (42) as follows[39]:

$$k_p \langle Q_k - Q_{k+1}, K \rangle = \frac{\Delta t}{2} k_p (\omega_{k+1} + \omega_k)^T S_K(Q_k). \tag{44}$$

Then using (44), the first difference $\Delta \mathcal{V}_k$ is obtained as

$$\Delta \mathcal{V}_k = \frac{1}{2}(\omega_{k+1} + \omega_k)^T [J(\omega_{k+1} - \omega_k) + \Delta t k_p S_K(Q_k)]. \tag{45}$$

Expanding the estimation error dynamics (38), which incorporates the compensation design of FTS-DO and includes the estimation error of the disturbance torque e_k^τ, yields the following expression:

$$(J + L_\omega)[\omega_{k+1} + \Delta t \, J^{-1} e_k^\tau] = (J - L_\omega)\omega_k - \Delta t k_p S_K(Q_k), \tag{46}$$

and rearranged as

$$J(\omega_{k+1} - \omega_k) + \Delta t k_p S_K(Q_k) = L_\omega(\omega_{k+1} + \omega_k) - \Delta t \, (\omega_{k+1} + \omega_k)^T \bar{C} e_k^\tau \tag{47}$$

where,

$$\bar{C} = (J + L_\omega)J^{-1}.$$

Substituting (47) in (45) gives the following expression for $\Delta \mathcal{V}$:

$$\Delta \mathcal{V}_k = -\frac{1}{2}(\omega_{k+1} + \omega_k)^T L_\omega(\omega_{k+1} + \omega_k) - \Delta t \, (\omega_{k+1} + \omega_k)^T \bar{C} e_k^\tau \tag{48}$$

$$\leq \frac{1}{2}(\omega_{k+1} + \omega_k)^T L_\omega(\omega_{k+1} + \omega_k) - \Delta t \, \|\omega_{k+1} + \omega_k\| \, \|\bar{C} e_k^\tau\|. \tag{49}$$

More conservative upper bounds on $\Delta \mathcal{V}_k$ may be obtained using the eigenvalue operators, as below:

$$\Delta \mathcal{V}_k \leq -\frac{1}{2}\lambda_{\min}(L_\omega)||\omega_{k+1} + \omega_k||^2 + \Delta t \, \lambda_{\max}(\bar{C})||\omega_{k+1} + \omega_k||||e_k^\tau||. \tag{50}$$

Imposing the condition that the aforementioned first difference is non-negative establishes conservative bounds for the convergence region of the attitude tracking error term $\omega_{k+1} + \omega_k$ as:

$$||\omega_{k+1} + \omega_k|| \leq \frac{\Delta t \lambda_{\max}(\bar{C})}{\lambda_{\min}(L_\omega)}||e_k^\tau||$$

$$\leq \frac{\Delta t \lambda_{\max}(\bar{C})}{\lambda_{\min}(L_\omega)} B^\tau. \tag{51}$$

as given in (40). □

Note that similar to the position tracking part in Section 4, the above result gives a conservative ultimate bound that is larger than the actual bounds of the neighborhood of the origin that attitude and angular velocity tracking errors may converge to.

6 | NUMERICAL SIMULATION

This section presents comprehensive numerical simulations of tracking control for an unmanned vehicle using the control laws presented in Proposition 3 and Proposition 4, along with the FTS disturbance observer in the inner loop as shown in Fig. 1 and Fig. 2. The controller tracks the trajectory of the vehicle in discrete time. Note that our approach uses the finite-time stable disturbance observer, which converges at a much faster rate than the outer loop with the asymptotically stable tracking controller.

The simulation is performed for a UAV quadcopter of mass $m = 4.34$ kg for a time period of $T = 10$ s with a time step size of $h = 0.01$ s, using the discrete-time LGVI model and the control laws (18) and (36). There are two scenarios studied here, both involving three-dimensional reference trajectories that are generated to pass between tall obstacles like trees or buildings in outdoor flights. The first scenario involves a figure eight-shaped reference trajectory with changes in height, as given by the following conditions:

$$b_k^r = [\sin(\frac{\pi}{2}t_k) \quad \sin(\frac{\pi}{2}t_k)\cos(\frac{\pi}{2}t_k) \quad 0.2\sin(\pi t_k) + \alpha t_k]^T.$$

Here α is the altitude gain of the trajectory to describe the change in height and is selected as $\alpha = \pi/4$, and

$$b_0 = [1 \; 1 \; 0]^T \text{m}, \quad v_0 = [0 \; 0 \; 0]^T \text{m/s},$$

$$R_0 = \mathbf{I}_{3\times3}, \quad \Omega_0 = [0 \; 0 \; 0]^T, \quad \Omega_0^r = [0 \; 0 \; 0]^T.$$

In the second scenario, a flight trajectory is studied that involves flying in between tall obstacles like high-rise buildings. This position trajectory is generated using an optimal LQR method that optimizes a combination of velocity, acceleration, and jerk[34], and is designed to pass through multiple desired waypoints. The position and velocity profiles of these trajectories are used in the control law (18).

The observer gains selected for the Hölder-continuous function $\mathcal{D}(e_k^\chi)$ for the disturbance observer in (13), are:

$$\lambda = 1.5 \text{ and } r = \frac{9}{7}.$$

and the initial estimates of disturbance force and torque are selected as $\widehat{\phi}_0^d = [9.3\ \ 13.6\ \ 8.2]^T\mathrm{N}$, and $\widehat{\tau}_0^d = [0.25\ \ 0.04\ \ 0.51]^T\mathrm{N.m}$, respectively. The control gains for the translational and rotational control laws in (18) and 36 are selected as follows:

$$P = 16\ \mathbf{I}_{3\times3};\ \ D = 0.07\ \mathbf{I}_{3\times3};\ \ L_\omega = 0.01\ \mathbf{I}_{3\times3};\ \ k_p = 1.01,$$

These gains are selected to achieve desired transient response characteristics, such that the settling time of the inner loop with the finite-time stable disturbance observer is small. In this case, these gain selections result in a settling time of less than 1 second for the inner loop FTS-DO, ensuring faster convergence of the disturbance observer compared to the outer loop tracking controller. The disturbance force and disturbance torque acting on the UAV in the inertial frame $\mathcal{I}$ are given by the following in this simulation:

$$\phi_k^d = \begin{bmatrix} 9 & + 2\sin(\pi t_k), \\ 10 & + 5\cos(\pi t_k), \\ 8 & + 3\sin(\pi t_k) \end{bmatrix}(\mathrm{N}),$$

and

$$\tau_k^d = \begin{bmatrix} 0.2\sin(\pi t_k) & + 0.3 \\ 0.2\cos(\pi t_k) & - 0.2 \\ 0.2\cos(\pi t_k) & + 0.3 \end{bmatrix}(\mathrm{N\cdot m})$$

The performance of the feedback controller in tracking the eight-shaped trajectory with and without disturbance correction terms in the force and torque control laws is shown in Fig. 3. In this figure, plots 3a and 3b present the results for the norms of position and velocity tracking errors, respectively. The attitude tracking error is parameterized by the principal rotation angle Φ_k of the attitude error matrix Q_k as $\Phi_k = \cos^{-1}\left(\frac{1}{2}(\mathrm{tr}(Q_k) - 1)\right)$. Plots in 3c and 3d indicate the rotational motion tracking errors. It is evident from the plots that in the presence of the disturbance force and torque, the FTS disturbance observer estimates the disturbances effectively and the tracking controller ensures that all translational and rotational tracking errors asymptotically converge to a neighborhood of zero. However, without the DO, the disturbance force and torque are not compensated well and tracking errors do not settle down to the desired neighborhood of the reference translational and rotational motions. The size of this neighborhood depends on the bounds of the disturbances and the gains selected, according to Theorem 1 and 2. In Fig. 3e and 3f, and 3g, the graphs depict the bounded convergence of $\|\tilde{b}_{k+1} - \tilde{b}_k\|$, $\|\tilde{v}_{k+1} + \tilde{v}_k\|$, and $\|\omega_{k+1} + \omega_k\|$, respectively, with the bounds given by Theorem 1 and Theorem 2. Figure 4 presents plots of the 3D trajectory and its projection on the xy-plane for the position trajectory of the UAV tracking the reference trajectory utilizing the feedback control laws (18) and (36). The plots indicate that the actual trajectory ultimately converges to a bounded neighborhood of the reference trajectory (with the bounds as mentioned above), and remains consistently stable throughout the simulated time duration.

Fig. 5 shows the performance of our feedback controller in tracking the second reference trajectory for a flight duration of 100s when the above disturbance force and torque are acting on the UAV, with and without the disturbance observer implemented in the inner loop. The norms of translational and rotational state tracking errors are presented in this figure. These results demonstrate that the presence of a disturbance force and torque is effectively countered by the FTS disturbance observer in the inner loop, leading to asymptotic convergence of both translational and rotational tracking errors within a desired neighborhood of the reference trajectory. In contrast, the absence of the FTS-DO fails to compensate for the disturbances, and tracking errors do not settle down to desired bounds of the position and velocity tracking errors. Fig. 6 displays two views of the time trajectory of the UAV tracking the reference trajectory using the feedback control laws (18) and 36. The plots clearly demonstrate that the actual trajectory converges to a bounded neighborhood of the reference trajectory and remains stable throughout the simulation.

7 | CONCLUSION AND FUTURE WORK

This study presents a robust trajectory tracking control scheme in discrete time for a rigid body with uncertain (gray box) dynamics due to unknown disturbance force and torque. The control scheme incorporates a Hölder-continuous FTS disturbance observer in the inner loop to estimate the disturbance inputs and compensate for them through the control laws. The position and attitude tracking control laws demonstrate nonlinear stability and robustness tracking of the reference trajectory while compensating for the disturbances in real time. The tracking errors are shown to ultimately converge to bounded neighborhoods of zero errors in an asymptotically stable manner. A comprehensive simulation study for the controller design with a disturbance observer is carried out for performance validation, and results are discussed. Future research directions are: (1) to obtain FTS tracking control laws for pose tracking that are more robust to disturbance inputs compared to asymptotically stable control laws;
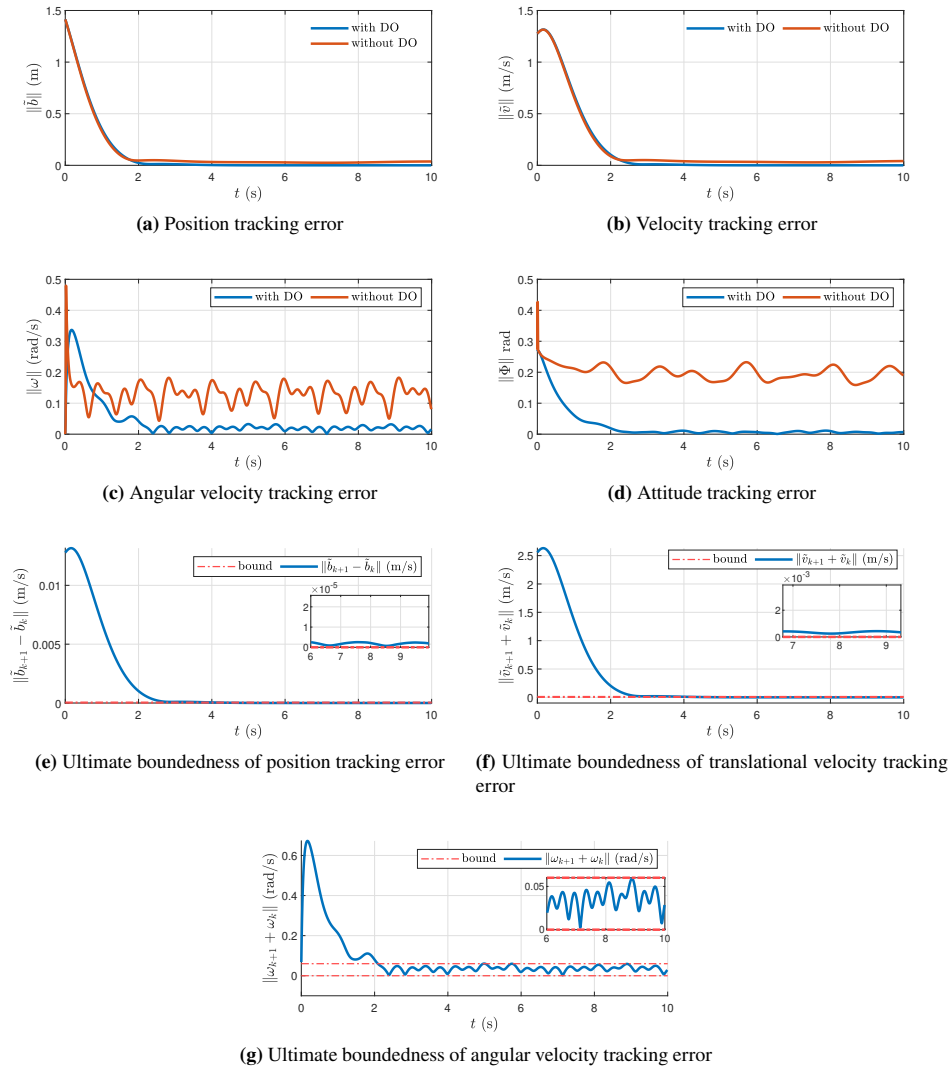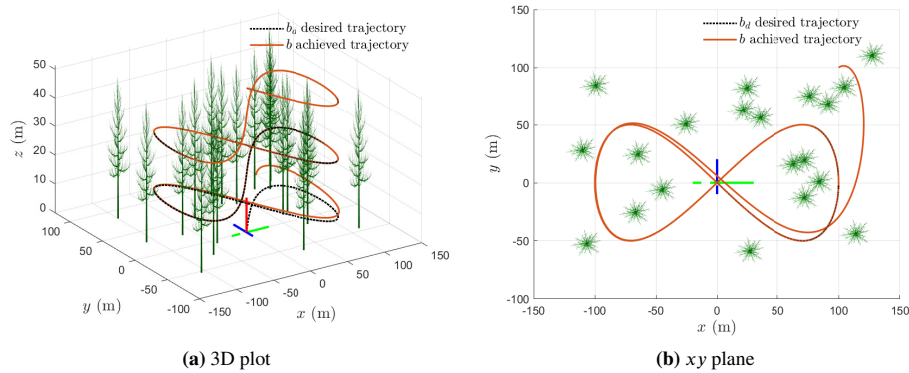
(a) Position tracking error

(b) Velocity tracking error

(c) Angular velocity tracking error

(d) Attitude tracking error

(e) Ultimate boundedness of position tracking error

(f) Ultimate boundedness of translational velocity tracking error

(g) Ultimate boundedness of angular velocity tracking error

FIGURE 3 Simulation Results

(a) 3D plot

(b) xy plane

FIGURE 4 Trajectory tracking with disturbance correction

(a) Position tracking error

(b) Velocity tracking error

(c) Angular velocity tracking error

(d) Attitude tracking error

FIGURE 5 Simulation Results

(a) 3D plot

(b) xy plane
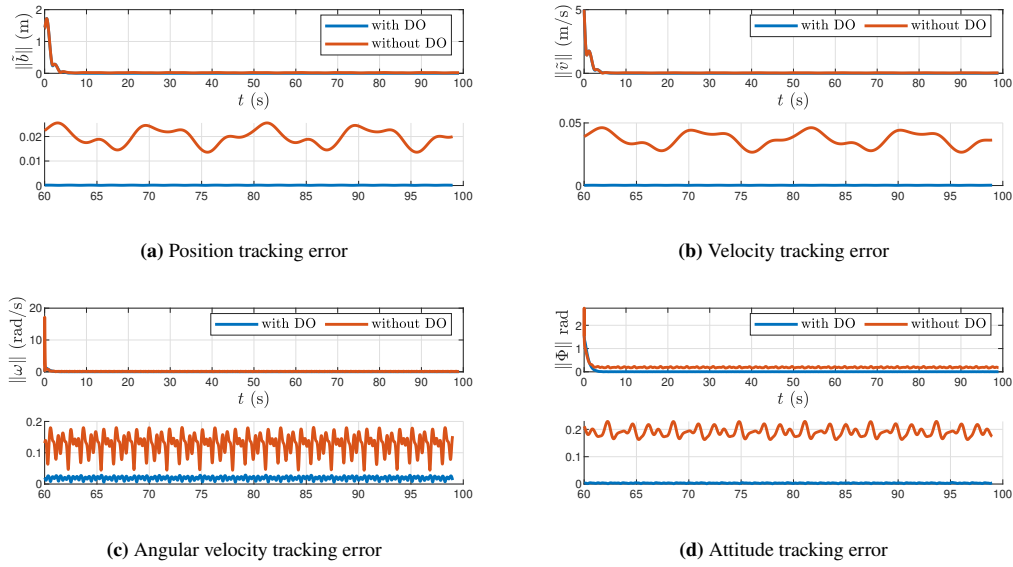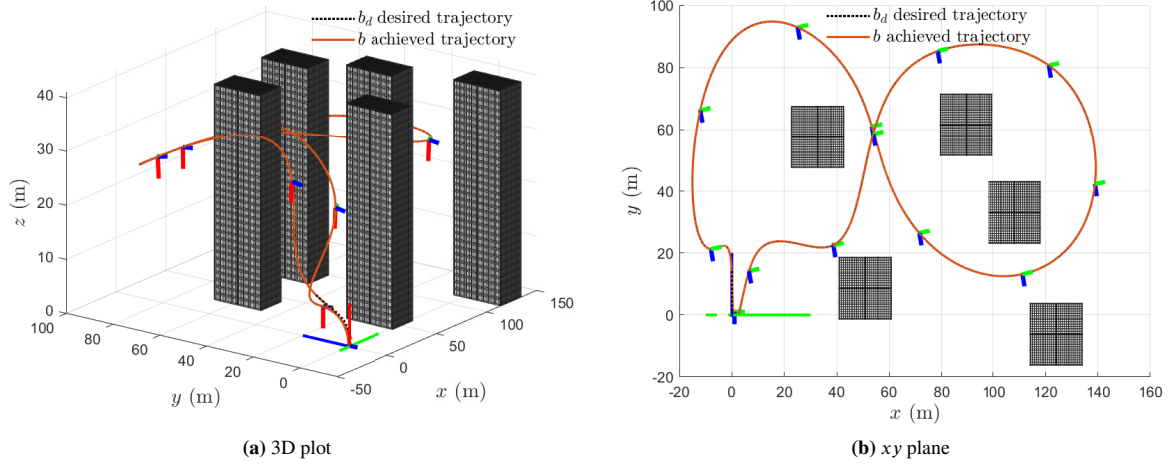
FIGURE 6 Trajectory tracking with disturbance correction

(2) to obtain LGVI discretization schemes with variable time step sizes that are more accurate in representing different time scales that may be present in the continuous-time dynamics; and (3) analysis of ultimate bounds on tracking control errors and estimation errors in the presence of disturbance forces and torques as well as measurement noise in measured outputs.

ACKNOWLEDGEMENT

References

1. Soderlund AA, Kumar M, Yang C. *Autonomous Wildfire Monitoring Using Airborne and Temperature Sensors in an Evidential Reasoning Framework*; AIAA Scitech 2019 Forum.

2. Soderlund AA, Kumar M, Aggarwal R. *Estimating the Real-time Spread of Wildfires with Vision-Equipped UAVs and Temperature Sensors via Evidential Reasoning*; AIAA Scitech 2020 Forum.

3. Hamrah R, Sanyal AK. Finite-time stable tracking control for an underactuated system in SE(3) in discrete time. *International Journal of Control* 2022; 95(4): 1106-1121. doi: 10.1080/00207179.2020.1841299

4. Hartlieb RJ. The cancellation of random disturbances in automatic control systems. *PhDT* 1956.

5. Shao X, Liu J, Cao H, Shen C, Wang H. Robust dynamic surface trajectory tracking control for a quadrotor UAV via extended state observer. *International Journal of Robust and Nonlinear Control* 2018; 28(7): 2700–2719.

6. Liu K, Wang R, Zheng S, Dong S, Sun G. Fixed-time disturbance observer-based robust fault-tolerant tracking control for uncertain quadrotor UAV subject to input delay. *Nonlinear Dynamics* 2022; 107(3): 2363–2390.

7. Mechali O, Xu L, Huang Y, Shi M, Xie X. Observer-based fixed-time continuous nonsingular terminal sliding mode control of quadrotor aircraft under uncertainties and disturbances for robust trajectory tracking: Theory and experiment. *Control Engineering Practice* 2021; 111: 104806.

8. Guo BZ, Zhao Zl. On the convergence of an extended state observer for nonlinear systems with uncertainty. *Systems & Control Letters* 2011; 60(6): 420–430.

9. Wang X, Sun S, Kampen vEJ, Chu Q. Quadrotor fault tolerant incremental sliding mode control driven by sliding mode disturbance observers. *Aerospace Science and Technology* 2019; 87: 417–430.

10. Cui L, Zhang R, Yang H, Zuo Z. Adaptive super-twisting trajectory tracking control for an unmanned aerial vehicle under gust winds. *Aerospace Science and Technology* 2021; 115: 106833.

11. Xia Y, Zhu Z, Fu M, Wang S. Attitude tracking of rigid spacecraft with bounded disturbances. *IEEE Transactions on Industrial Electronics* 2010; 58(2): 647–659.

12. Chen WH. Nonlinear disturbance observer-enhanced dynamic inversion control of missiles. *Journal of Guidance, Control, and Dynamics* 2003; 26(1): 161–166.

13. Chen WH, Yang J, Guo L, Li S. Disturbance-Observer-Based Control and Related Methods—An Overview. *IEEE Transactions on Industrial Electronics* 2016; 63(2): 1083-1095. doi: 10.1109/TIE.2015.2478397

14. Lee D. Nonlinear disturbance observer-based robust control of attitude tracking of rigid spacecraft. *Nonlinear Dynamics* 2017; 88: 1317-1328.

15. Asignacion A, Suzuki S, Noda R, Nakata T, Liu H. Frequency-Based Wind Gust Estimation for Quadrotors Using a Nonlinear Disturbance Observer. *IEEE Robotics and Automation Letters* 2022; 7(4): 9224–9231.

16. Basile G, Marro G. On the observability of linear, time-invariant systems with unknown inputs. *Journal of Optimization theory and applications* 1969; 3: 410–415.

17. Chen M, Xiong S, Wu Q. Tracking Flight Control of Quadrotor Based on Disturbance Observer. *IEEE Transactions on Systems, Man, and Cybernetics: Systems* 2021; 51(3): 1414-1423. doi: 10.1109/TSMC.2019.2896891

18. Bhale P, Kumar M, Sanyal AK. Finite-time stable disturbance observer for unmanned aerial vehicles. In: 2022 American Control Conference (ACC). ; 2022: 5010-5015

19. Hamrah R, Sanyal AK. Stable and Robust Position Tracking Control of Unmanned Vehicles Using A Finite-time Stable Disturbance Observer. In: 62nd IEEE Conference on Decision and Control (CDC), Dec. 13-15, 2023, Singapore. ; submitted.

20. Yim J, You S, Lee Y, Kim W. Chattering Attenuation Disturbance Observer for Sliding Mode Control: Application to Permanent Magnet Synchronous Motors. *IEEE Transactions on Industrial Electronics* 2023; 70(5): 5161-5170. doi: 10.1109/TIE.2022.3189074

21. Acary V, Brogliato B, Orlov YV. Chattering-Free Digital Sliding-Mode Control With State Observer and Disturbance Rejection. *IEEE Transactions on Automatic Control* 2012; 57(5): 1087-1101. doi: 10.1109/TAC.2011.2174676

22. Lee T, Leok M, Mcclamroch N. Lie group variational integrators for the full body problem in orbital mechanics. *Celestial Mechanics and Dynamical Astronomy* 2007; 98: 121-144. doi: 10.1007/s10569-007-9073-x

23. Nordkvist N, Sanyal AK. A Lie group variational integrator for rigid body motion in SE(3) with applications to underwater vehicle dynamics. In: 49th IEEE Conference on Decision and Control (CDC). ; 2010: 5414–5419

24. Hamrah R, Sanyal AK, Viswanathan SP. Discrete Finite-time Stable Attitude Tracking Control of Unmanned Vehicles on SO(3). In: 2020 American Control Conference (ACC). ; 2020: 824-829

25. Hairer E, Lubich C, Wanner G. *Geometric numerical integration*. 31 of *Springer Series in Computational Mathematics*. Springer-Verlag, Berlin. second ed. 2006. Structure-preserving algorithms for ordinary differential equations.

26. Benettin G, Giorgilli A. On the Hamiltonian interpolation of near-to-the identity symplectic mappings with application to symplectic integration algorithms. *Journal of Statistical Physics* 1994; 74: 1117–1143.

27. Viswanathan SP, Sanyal AK, Samiei E. Integrated Guidance and Feedback Control of Underactuated Robotics System in SE(3). *Journal of Intelligent and Robotic Systems* 2018; 89(1-2): 251–263.

28. Bloch A, Baillieul J, Crouch P, Marsden J. *Nonholonomic Mechanics and Control, ser. Interdisciplinary Applied Mathematics*. Springer, Verlag . 2003.

29. Bullo F, Lewis AD. *Geometric Control of Mechanical Systems*. 49 of *Texts in Applied Mathematics*. Springer Verlag . 2004.

30. Murray RM. *A Mathematical Introduction to Robotic Manipulation*. CRC Press . 1994.

31. Nordkvist N, Sanyal AK. A Lie Group Variational Integrator for Rigid Body Motion in SE(3) with Applications to Underwater Vehicle Dynamics. In: 49th IEEE Conference on Decision and Control (CDC). IEEE; 2010: 5414-5419.

32. Cortez AC, Ford BT, Nayak I, Narayanan S, Kumar M. *Path Planning for a Dubins Agent with Resource Constraints and Dynamic Obstacles*; AIAA SCITECH 2023 Forum.

33. Ford BT, Aggarwal R, Kumar M, Manyam SG, Casbeer D, Grymin D. *Backtracking Hybrid A* for Resource Constrained Path Planning*; AIAA SCITECH 2022 Forum.

34. Dhullipalla MH, Hamrah R, Warier RR, Sanyal AK. Trajectory Generation on SE(3) for an Underactuated Vehicle with Pointing Direction Constraints. In: 2019 American Control Conference (ACC). ; 2019: 1930-1935

35. Eslamiat H, Li Y, Wang N, Sanyal AK, Qiu Q. Autonomous Waypoint Planning, Optimal Trajectory Generation and Nonlinear Tracking Control for Multi-rotor UAVs. In: 18th European Control Conference (ECC). ; 2019: 2695-2700

36. Eslamiat H, Sanyal AK, Lindsay C. Discrete Time Optimal Trajectory Generation and Transversality Condition with Free Final Time. In: 2021 International Conference on Unmanned Aircraft Systems (ICUAS). ; 2021: 843-852

37. Aggarwal S, Kumar N. Path planning techniques for unmanned aerial vehicles: A review, solutions, and challenges. *Computer Communications* 2020; 149: 270-299. doi: https://doi.org/10.1016/j.comcom.2019.10.014

38. Lee T, Leok M, McClamroch NH. Geometric tracking control of a quadrotor UAV on SE(3).. In: 49th IEEE Conference on Decision and Control (CDC). IEEE; 2010: 5420–5425.

39. Hamrah R, Warier RR, Sanyal AK. Discrete-time Stable Tracking Control of Underactuated Rigid Body Systems on SE(3). In: 57th IEEE Conference on Decision and Control (CDC). ; 2018: 2932–2937.